



Colorless polyimides from 2,2',3,3'-biphenyltetracarboxylic dianhydride and fluorinated diamines

Yuanzhen Xu^{a,b}, Mengru Zhang^b, Yuanyuan Pang^c, Tianyue Zheng^b, Li Zhang^a, Zhen Wang^{b,*}, Jingling Yan^{b,*}

^a School of Materials Science & Chemical Engineering, Ningbo University, Ningbo 315211, China

^b Ningbo Institute of Materials Technology & Engineering, Chinese Academy of Science, Ningbo 315201, China

^c College of Science & Technology, Ningbo University, Cixi 315300, China

ARTICLE INFO

Keywords:

Colorless polyimide
2,2',3,3'-Biphenyltetracarboxylic dianhydride
Fluorinated diamine
Optical transparency
Glass transition temperature

ABSTRACT

In this work, 2,2',3,3'-biphenyltetracarboxylic dianhydride (3,3'-BPDA) was exploited to produce colorless polyimides (CPIs), and their properties were systematically investigated. High-temperature polycondensation of 3,3'-BPDA with fluorinated diamines enabled the synthesis of CPIs with high molecular weights. The resulting CPIs displayed deficient chain packing owing to the steric hindrance and suppressed formation of charge transfer complexes (CTC), as confirmed by the interchain distances (5.9–6.7 Å). These CPIs were highly soluble in common organic solvents due to the enlarged interchain distances. Depending on the chain rigidity, the glass transition temperatures of the CPIs ranged from 287 to 414 °C. More importantly, these CPIs exhibited outstanding optical properties, with a cut-off wavelength of 355–370 nm, transmittance at 450 nm of 79.6–89.2%, and yellow index of 1.4–13.4.

1. Introduction

Aromatic polyimides are widely used in aerospace, microelectronics, and transportation industries due to their excellent high-temperature resistance, outstanding mechanical properties, and low dielectric constants and loss factors.[1–4] However, the deep color of conventional polyimides hampers their applications in optics and optoelectronics,[5] where high optical transparency is required in applications like cover window films, touch screen panels, and thin film transistor substrates, replacing fragile, thick, and heavy inorganic glass counterparts.[6–8] Therefore, considerable research efforts have been devoted to reducing or even eliminating the deep color of polyimides without compromising their other desirable properties.

The yellowish to brown color of polyimides originates from their conjugated aromatic backbones and the formation of charge-transfer complexes (CTC).[6,9,10] Consequently, CPIs are often achieved by interrupting conjugation, enlarging interchain distances, reducing the electron-donating capability of diamines, or decreasing the electron-withdrawing capability of dianhydrides.[10] Efficient structural manipulation strategies include the incorporation of fluorinated monomers, aliphatic moieties, non-coplanar segments, flexible linkages, and

bent architectures.[11–21] For instance, polyimides derived from fluorinated monomers exhibit significantly improved optical transparency while retaining excellent thermal and mechanical properties.[22] In particular, polyimides made from 4,4'-(hexafluoroisopropylidene)diphthalic anhydride (6FDA) and 2,2'-bis(trifluoromethyl)benzidine (TFMB) showed excellent optical transparency, high glass transition temperature (T_g), and favorable mechanical robustness.[23–27] Such enhancements can be contributed to the high electronegativity of CF_3 substituents in TFMB, as well as the disruption of conjugation caused by the bulky hexafluoroisopropylidene segments in 6FDA and the twisted 2,2'-disubstituted biphenyl moieties in TFMB. However, the use of 6FDA and TFMB leads to high cost, inferior dimensional stability, low modulus and poor solvent resistance of the resulting CPIs. To overcome such limitations, Hasegawa *et al.*[14] developed CPIs with high modulus and low coefficients of thermal expansion (CTE) by using amide-containing monomers, and by rationally adjusting the compositions of the dianhydride and diamines monomers. Besides 6FDA and TFMB, fluorinated ladder dianhydrides were also prepared by Auman *et al.*[28] and Tu *et al.*[29] and the resulting CPIs displayed reduced CTE and enhanced mechanical properties. However, the synthesis of fluorinated monomers involves multi-step reactions and complicated purification procedures,

* Corresponding authors.

E-mail addresses: wz@nimte.ac.cn (Z. Wang), jyan@nimte.ac.cn (J. Yan).

<https://doi.org/10.1016/j.eurpolymj.2022.111528>

Received 12 June 2022; Received in revised form 4 August 2022; Accepted 21 August 2022

Available online 31 August 2022

0014-3057/© 2022 Elsevier Ltd. All rights reserved.

leading to high costs. From the viewpoint of cost and performance balance, current commercial aromatic dianhydrides for CPI production are limited to 6FDA. Thus, it is of practical significance to develop CPIs with desired properties and low cost, using alternative dianhydrides other than 6FDA.

2,2',3,3'-Biphenyltetracarboxylic dianhydride (3,3'-BPDA) features a rigid but non-coplanar architecture because of the steric hindrance of *ortho*-substituted phthalic anhydride units with the dihedral angle of 63°. Its electron affinity (E_a), an indicator of electron-withdrawing ability, is significantly lower than 6FDA (1.87 versus 2.21 eV), according to Ando's report. [30] Thus, it can be anticipated that 3,3'-BPDA-based polyimides could exhibit reduced coloration due to the interrupted conjugation and reduced CTC formation. Furthermore, 3,3'-BPDA can potentially be manufactured at a low cost since its synthetic route is similar to that of the conventional 3,3',4,4'-biphenyltetracarboxylic dianhydride (4,4'-BPDA). In this respect, Tong *et al.* [31] first prepared 3,3'-BPDA through Ullman coupling of 3-iodophthalate, and demonstrated that polyimides from 3,3'-BPDA had lower molecular weights, higher T_g , low crystallinity and enhanced solubility when compared to their counterparts from 4,4'-BPDA. The lower molecular weights of 3,3'-BPDA-derived polyimides were related to the reduced polymerizability caused by the steric hindrance, as well as the tendency to form cyclic oligomers. Meanwhile, the higher T_g and enhanced solubility can be attributed to the restricted chain motions caused by the twisted and non-coplanar structures. Goto *et al.* [32] synthesized 3,3'-BPDA by Ni-catalyzed coupling of 3-chlorophthalimide. They found that the polyimide films from 3,3'-BPDA and rigid diamines were highly brittle due to the reduced molecular weights. However, copolymers from 3,3'-BPDA, 4,4'-BPDA and TFMB were flexible with excellent optical transparency. Yokota *et al.* [33–35] investigated the isomeric effects of BPDAs on the viscoelasticity of polyimides. The results revealed that 3,3'-BPDA-derived polyimides showed higher T_g , lower β relaxation temperatures (T_β) and intensities, and reduced rubbery plateau regions when compared to 4,4'-BPDA-derived ones. Our group developed colorless homo- and co-polyimides from 3,3'-BPDA, hydrazine, and commercial aromatic dianhydrides. The obtained polyimides exhibited extremely high T_g (371–432 °C) and outstanding optical transparency. [36] Our group also demonstrated that imide oligomers and thermosets based on 3,3'-BPDA exhibited improved processability, and thermal and mechanical properties than the benchmark oligomer TriA-X. [37] However, no reports dealing with CPIs using 3,3'-BPDA as the mere dianhydride monomer have so far been published, owing to the difficulties in achieving high-molecular-weight polyimides.

Herein, we report a set of CPIs based on 3,3'-BPDA and fluorinated diamine monomers. The thermal, mechanical and optical properties of the CPIs were systematically investigated, and their structure-property relationship was elucidated.

2. Experimental

2.1. Materials

TFMB, 2,2'-bis(trifluoromethyl)-4,4'-diaminodiphenyl ether (6FODA), 1,4-bis(4-amino-2-trifluoromethylphenoxy)benzene (6FAPB), 2,2-bis[4-(4-aminophenoxy)phenyl]-hexafluoropropane (HFBAPP), 4,4'-bis[4-amino-2-(trifluoromethyl)phenoxy]biphenyl (6FAPBP), 4,4'-diaminobenzanilide (DABA), 2,2'-dimethylbenzidine (DMBZ), and 9,9-bis(3-fluoro-4-aminophenyl) fluorene (FFDA) were obtained from Chinatech Co. Ltd. (Tianjin, China), and used without further purification. All other chemicals were purchased from Aladdin Corporation (Shanghai, China) and used as received unless otherwise specified. *N*-methyl-2-pyrrolidinone (NMP) and *m*-cresol were purified by vacuum distillation over calcium hydride. 3,3'-BPDA was prepared according to literature procedures, [32] and then purified by sublimation in vacuum.

2.2. CPI syntheses

The polyimides were synthesized via a traditional one-step-method in *m*-cresol. The monomer concentrations were kept at ~30 wt%, and catalyst loading was fixed to 0.1 mol equivalent to anhydride. A typical example of synthesis is shown below.

TFMB (0.3202 g, 1.0 mmol), 3,3'-BPDA (0.2942 g, 1.0 mmol), benzoic acid (0.0244 g, 0.2 mmol), isoquinoline (0.0235 g, 0.2 mmol), and *m*-cresol (1.5 mL) were charged into a flask with an overhead stirrer. The reaction was heated at 90 °C for 1 h, and then at 180 °C for 10 h under nitrogen. The reaction was then diluted with *m*-cresol (5 mL) and poured into ethanol (20 mL). The obtained solid was collected, Soxhlet extracted with ethanol for 24 h, and dried under vacuum for 12 h at 120 °C to yield 3,3'-BPDA/TFMB (0.5785 g, yield: 94%).

2.3. Film preparation

The CPI films were prepared from the corresponding *N,N*-dimethylacetamide (DMAc, ~6 wt%) solutions. The polymers were dissolved in DMAc, and the solutions were filtered through a 1 μ m GF filter and cast on a glass substrate. DMAc was removed by heating at 60 °C for 4 h in an oven, and then heated at 100 °C/1h, 150 °C/1h, 200 °C/1h, 250 °C/1h, and 300 °C/1h under vacuum. After cooling down, the films were peeled off by immersing in water, and then dried at 110 °C for 2 h. The thickness of the films was ~30 μ m.

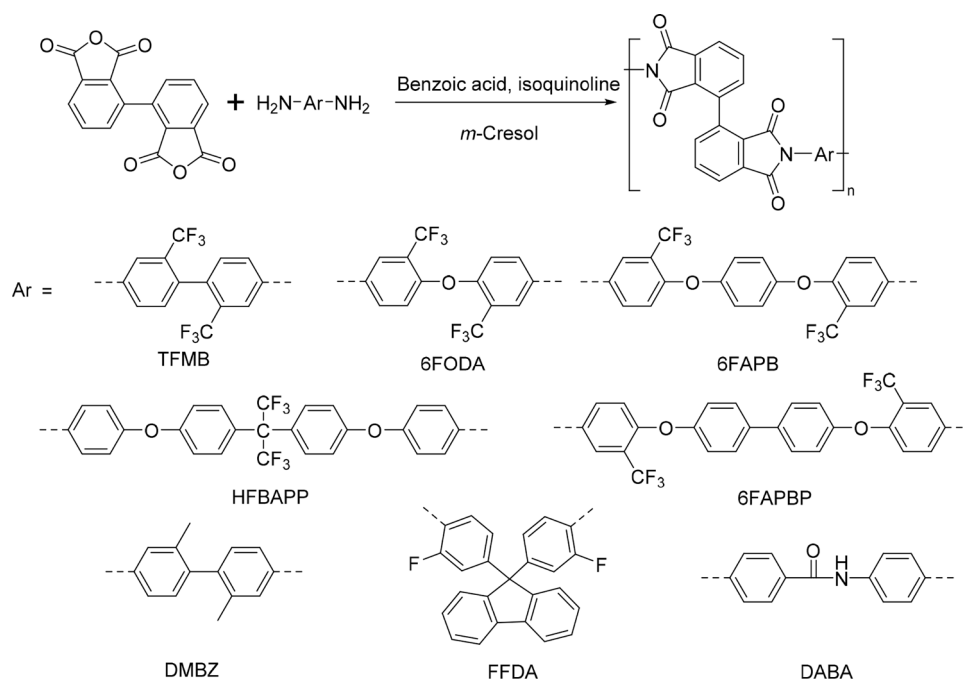
2.4. Characterization

Fourier transform infrared (FTIR) spectra were obtained on a Cary660+620 Micro FTIR instrument (Agilent, USA). ^1H NMR spectra were obtained on a Bruker Advance neo 600 Spectrometer (Bruker, Germany). Gel permeation chromatography (GPC) was carried out on a TOSOH HLC-8420 GPC (Tosoh, Japan) equipped with a refractive-index detector. Wide-angle X-ray diffraction (WAXD) was performed using a Bruker D8 Advance Davinci instrument (Bruker Germany) with Cu K α radiation at a wavelength (λ) of 1.54 Å. Glass transition behavior was studied using a Q850 DMA (TA Instruments, USA) at a heating rate of 5 °C min $^{-1}$. Thermogravimetric analysis (TGA) was performed on a Q55 TGA (TA Instruments, USA) at a heating rate of 10 °C min $^{-1}$ in nitrogen. CTE was measured with TMA Q400EM (TA Instruments, USA) at a heating rate of 5 °C min $^{-1}$ from 100 to 200 °C. Tensile testing was performed on a Zwick/Roell Z1.0 universal material testing machine (ZwickRoell GmbH&Co.KG, Germany) with a constant displacement rate of 2 mm min $^{-1}$. UV-vis spectra were measured on a Lambda 950 spectrometer (Perkin-Elmer, USA) under transmittance mode. Color intensity was assessed on an UltraScan VIS Hunter lab instrument (Hunter Lab, USA) according to CIE (Commission International de l'Eclairage) standard D65 illuminant at an observational angle of 10°.

3. Results and discussion

3.1. CPI syntheses

3,3'-BPDA exhibits low polymerizability against aromatic diamines due to its sterically hindered structure and tendency to form cyclic oligomers. Consequently, it is difficult to achieve high-molecular-weight poly(amic acid)s (PAA) from 3,3'-BPDA and rigid diamines via conventional two-step method, and the resulting polyimides are highly brittle. Polyimide films derived from 3,3'-BPDA and flexible ether-containing diamines are creasable despite their low molecular weights. The molecular weights of 3,3'-BPDA-derived polyimides can be increased by high-temperature polycondensation in *m*-cresol. Goto *et al.* reported that copolymers synthesized from 3,3'-BPDA, 4,4'-BPDA and TFMB were flexible and colorless. [32] However, no reports dealing with homo-polymers from 3,3'-BPDA and fluorinated diamines have been thus far published.



Scheme 1. Synthesis of 3,3'-BPDA-derived CPIs.

Table 1

Monomer composition, molecular weights, polydispersity, and fluorine contents of 3,3'-BPDA-derived CPIs.

CPI	Monomer composition	M_n (kg mol ⁻¹) ^a	M_w (kg mol ⁻¹) ^a	PDI ^a	Fluorine content (%)
CPI-1	3,3'-BPDA/TFMB	81	165	2.04	19.7
CPI-2	3,3'-BPDA/6FODA	90	260	2.89	19.2
CPI-3	3,3'-BPDA/6FAPB	170	490	2.88	16.6
CPI-4	3,3'-BPDA/HFBAPP	66	223	3.38	14.8
CPI-5	3,3'-BPDA/6FAPBP	46	124	2.70	14.9
CPI-6	3,3'-BPDA/TFMB (0.4)/DMBZ(0.6)	- ^b	- ^b	- ^b	8.3
CPI-7	3,3'-BPDA/TFMB (0.5)/FFDA(0.5)	97	260	2.68	16.4
CPI-8	3,3'-BPDA/TFMB (0.5)/DABA(0.5)	39	100	2.56	14.8

^a Measured by GPC using DMF as the eluent at a flowrate of 0.2 mL min⁻¹. M_n : number average molecular weights; M_w : weight average molecular weights; PDI: polydispersity.

^b Not measured because it is insoluble in DMF.

Herein, a set of CPIs were synthesized from 3,3'-BPDA and fluorinated diamines through an one-step method in *m*-cresol (Scheme 1). Achieving high molecular weights required high 3,3'-BPDA purity (purified by sublimation), high monomer concentration (~30 wt%), and proper catalysts (benzoic acid and isoquinoline, 0.1 M equivalent to anhydride). The polymerization of 3,3'-BPDA with TFMB, 6FODA, 6FAPB, HFBAPP, and 6FAPBP proceeded smoothly due to the good solubility of the resulting CPIs in *m*-cresol. In contrast, polymers from DABA, DMBZ, and FFDA were insoluble in *m*-cresol, leading to premature precipitation and thus relatively lower molecular weights. Hence, TFMB was used as a co-monomer to improve the solubility, and high-molecular-weight co-polyimides were achieved by adding 40–50% (molar percentage) TFMB. The weight average molecular weights and polydispersity of these CPIs were 100–490 kg mol⁻¹ and 2.04–3.88,

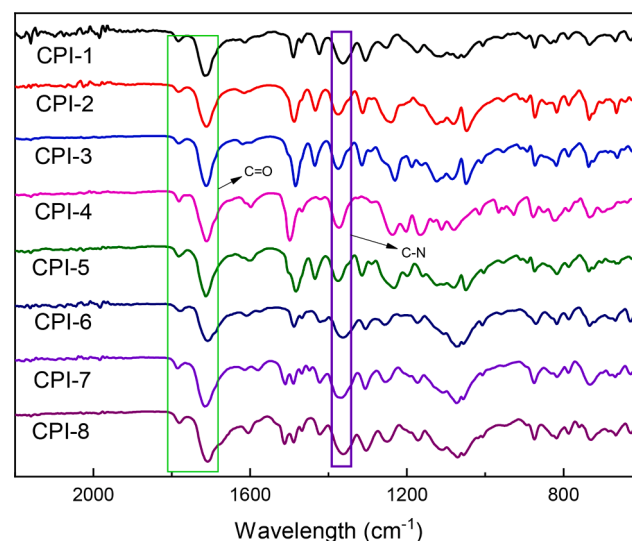
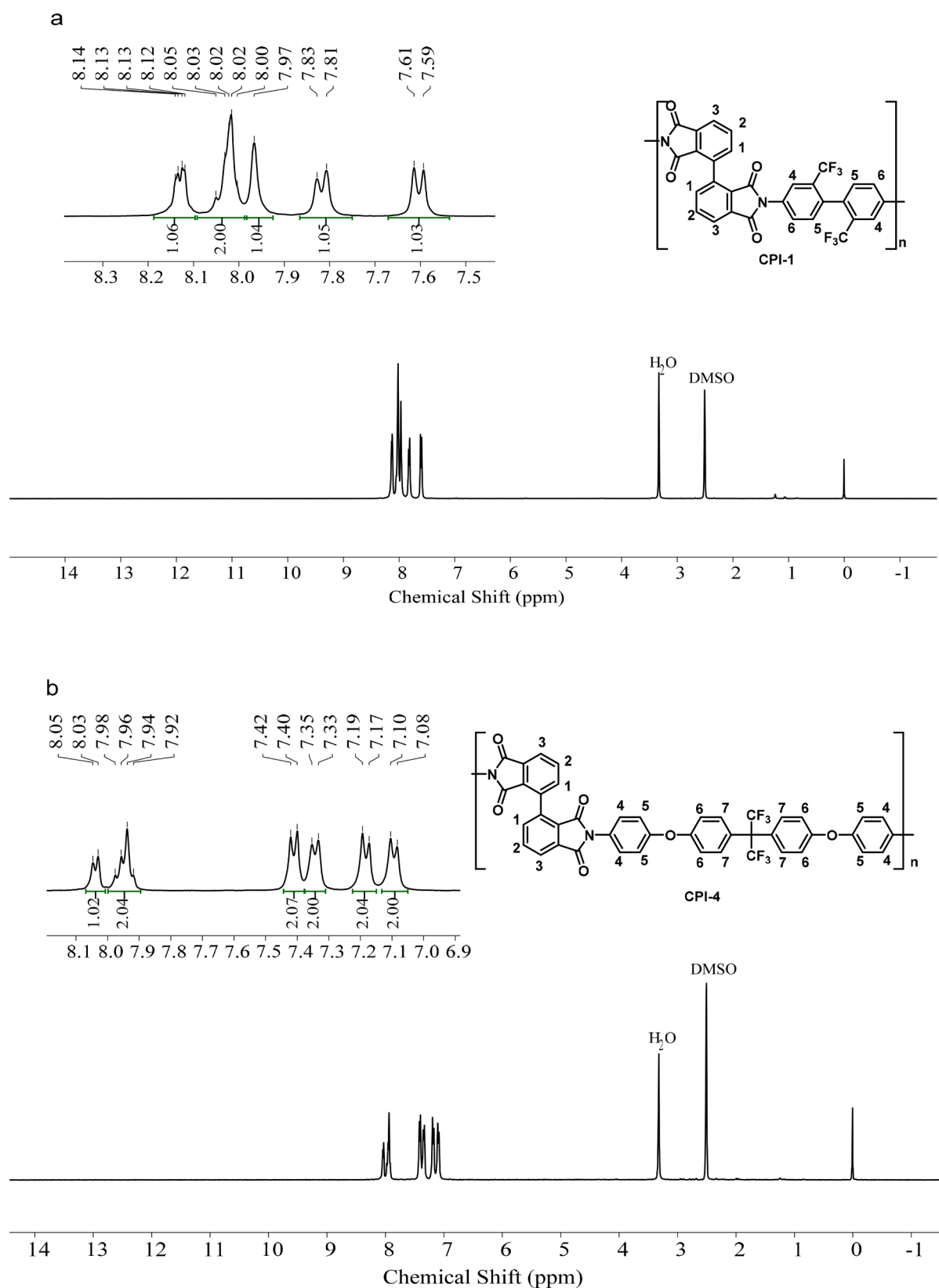


Fig. 1. FT-IR spectra of 3,3'-BPDA-derived CPIs.

respectively (Table 1). Furthermore, all CPI films were robust, transparent, and creasable.

The structures of these polymers were studied by ¹H NMR and FT-IR. In the FT-IR spectra (Fig. 1), the peaks at ~1780 cm⁻¹ (asymmetric C=O stretching), ~1720 cm⁻¹ (symmetric C=O stretching), and 1380 cm⁻¹ (C-N stretching) were assigned to the imide rings, while those at ~1140 cm⁻¹ (symmetric F-C-F stretching) and 1250 cm⁻¹ (asymmetric F-C-F stretching) were attributed to the fluorinated substituents (Fig. 1). In the ¹H NMR spectrum of CPI-1, the features at 8.13 and 8.01 ppm represented the aromatic protons in 3,3'-BPDA residues, while those at 7.96, 7.82 and 7.61 ppm were related to TFMB residues (Fig. 2a). Similar results were observed for CPI-4, with the features at 7.41, 7.34, 7.19 and 7.10 ppm assigned to HFBAPP residues (Fig. 2b). Furthermore, the integral ratios of these peaks agreed well with the calculated values.



3.2. Morphology

The chain packing profiles of 3,3'-BPDA-derived CPIs were studied by WAXD. All CPIs in this study were amorphous, reflected by their

broad diffraction peaks (Fig. 3). The interchain distances (d -spacing) of these polymers were 5.9–6.7 Å, which were larger than those of reported conventional polyimides.[26,38] This can be explained by their deficient chain packing caused by the rigid and contorted 3,3'-BPDA

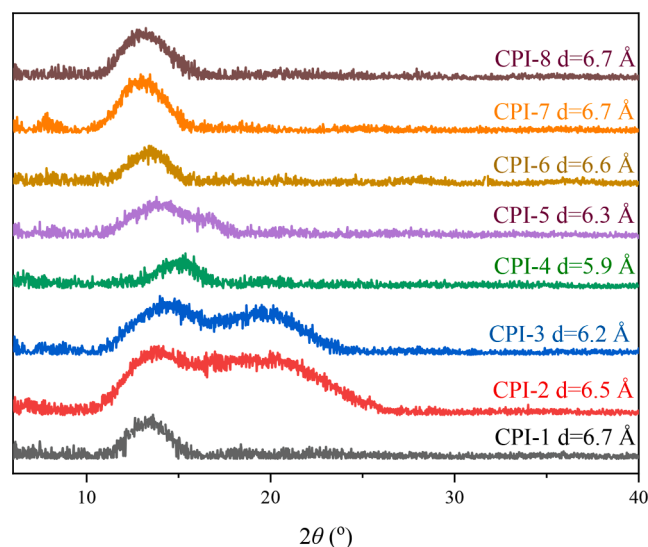


Fig. 3. WAXD patterns of 3,3'-BPDA-derived CPIs.

residues, as well as bulky F or CF₃ substituents. CPIs with flexible linkages exhibited higher segmental mobility, facilitating efficient chain packing and leading to lower *d*-spacing values. From CPI-1 to CPI-4, with the increments of ether contents, the interchain distances decreased from 6.7 Å to 5.9 Å. In contrast, CPIs from rigid diamines (TFMB, FFDA, and DMBZ) demonstrated more restricted segmental motions, thereby enlarged interchain distances. Two diffraction peaks were detected for CPI-2 (3,3'-BPDA/6FODA) and CPI-3 (3,3'-BPDA/6FAPB), which can respectively be attributed to average interchain distances and π - π stacking interactions due to the enhanced conjugation.

3.3. Solubility

The solubility of the 3,3'-BPDA-derived CPIs was measured in different organic solvents. These CPIs exhibited good solubility in NMP, DMAc, DMF, DMSO, and *m*-cresol (Table S1). Furthermore, some polymers were even soluble in dioxane, chloroform and tetrahydrofuran. Two factors accounted for the enhanced organic solvent solubility of these CPIs. First, the twisted, sterically hindered architecture and reduced electron-withdrawing capability of 3,3'-BPDA residues suppressed dense chain packing and decreased the inter- and intra-molecular interactions. Second, fluorinated diamine residues further frustrated dense chain packing and weakened inter- and intra-molecular interactions in these polymers. The latter was due to the combined effects of decreased electron-donating ability caused by the electronegative fluorine atoms, low polarity of C-F bonds, and/or bulky CF₃

substituents. The CPIs from TFMB, 6FODA, 6FAPB, HFBAPP, and 6FAPBP moieties showed similar solubility due to similarity in their structures. The co-polyimides from DMBZ, DABA, and FFDA exhibited lower solubility due to their lower fluorine contents. In particular, CPI-8 (3,3'-BPDA/TFMB/DABA) was insoluble in low boiling solvents due to the presence of additional hydrogen bonding interactions in the amide segments.

3.4. Thermal properties

TGA measurements were used to study the thermal stability of 3,3'-BPDA-derived CPIs in nitrogen. The 5% weight loss temperatures (*T*_{5%}) of these polymers were 516–579 °C in nitrogen (Table 2 and Figure S1), reflecting excellent thermal stability. For certain diamines, 3,3'-BPDA-derived CPIs exhibited higher thermal stability than reported 6FDA-derived ones, due to the absence of hexafluoroisopropylidene moieties in the dianhydride residues.[3,39] CPI-1 (3,3'-BPDA/TFMB) exhibited the best thermal stability due to the lack of heteroatoms in its backbone. In contrast, the CPIs derived from HFBAPP, DMBZ, and DABA showed inferior thermal stability due to the existence of hexafluoroisopropylidene, methyl and amide groups, respectively, which were more susceptible to thermal decomposition.

The relaxation behaviors of the 3,3'-BPDA-derived CPIs were investigated by DMA measurements. The *T*_g of these polyimides spanned a range of 287–414 °C (Table 2 and Fig. 4), largely dictated by their chain rigidity. For given diamines, the *T*_g values of 3,3'-BPDA-derived CPIs were ~20 °C higher than those of 6FDA-derived ones due to their higher chain rigidity.[3,39] The CPIs from 6FAPB, HFBAPP, and 6FAPBP exhibited lower *T*_g values due to their higher ether contents and lower imide concentrations. By comparison, the CPIs from TFMB, DMBZ, FFDA, and DABA showed markedly higher *T*_g values due to the lack of flexible linkages. CPI-7 (3,3'-BPDA/TFMB/FFDA) displayed the highest *T*_g because of the bulky cardo architecture of fluorene segments. The *T*_g of 3,3'-BPDA/TFMB/DMBZ was ~20 °C greater than that of 3,3'-BPDA/TFMB. This could be attributed to the smaller size of methyl substituents relative to trifluoromethyl groups, which induced a lower interchain distance. 3,3'-BPDA/TFMB/DABA also displayed higher *T*_g than 3,3'-BPDA/TFMB, owing to the additional hydrogen bonding interactions in the amide groups. Besides primary transitions, obvious β transitions were also observed in the CPIs from TFMB, 6FODA, and DMBZ. The sub-*T*_g relaxation was related to the local segmental motions of sterically hindered 2,2'-disubstituted biphenyl or 2,2'-disubstituted diphenyl ether moieties. The temperatures and magnitudes of the β transitions in TFMB-derived CPIs were significantly higher than those of the DMBZ and 6FODA-derived ones, caused by the larger size of CF₃ relative to CH₃, or higher rigidity of biphenyl relative to diphenyl ether. As expected, the magnitudes of β transitions in TFMB-derived copolymers were considerably lower than that in 3,3'-BPDA/TFMB.

The dimensional stability of 3,3'-BPDA-derived CPIs was evaluated

Table 2
Thermal and mechanical properties of 3,3'-BPDA-derived CPIs.

CPI	Modulus (GPa)	Tensile strength (MPa)	Elongation-at-break (%)	<i>T</i> _g (°C) ^a	<i>T</i> _{5%} (°C) ^b	CTE (ppm K ⁻¹) ^c
CPI-1	2.3 ± 0.24	63 ± 0.7	3.0 ± 0.4	382	579	68
CPI-2	1.9 ± 0.04	74 ± 1.5	5.1 ± 0.7	315	553	66
CPI-3	1.9 ± 0.16	77 ± 3.6	5.5 ± 0.6	287	564	69
CPI-4	1.9 ± 0.09	92 ± 5.2	7.2 ± 0.7	287	534	61
CPI-5	1.8 ± 0.06	86 ± 7.1	7.0 ± 1.6	294	562	70
CPI-6	2.4 ± 0.07	72 ± 1.4	3.3 ± 0.2	401	516	72
CPI-7	2.4 ± 0.08	64 ± 3.8	3.0 ± 0.2	414	558	65
CPI-8	2.0 ± 0.20	78 ± 6.8	4.9 ± 0.5	405	532	62
6FDA-TFMB[39]	1.7	98	11.6	358	530	68
6FDA-DMBz[39]	1.8	111	9.6	386	510	56
6FDA-HFBAPP[3]	2.0	87	16	263		51

^a Measured by DMA at a heating rate of 5 °C min⁻¹ and a frequency of 1 Hz.

^b Measured by TGA at a heating rate of 10 °C min⁻¹ under N₂.

^c Measured by TMA at a heating rate of 5 K min⁻¹ from 100 to 200 °C.

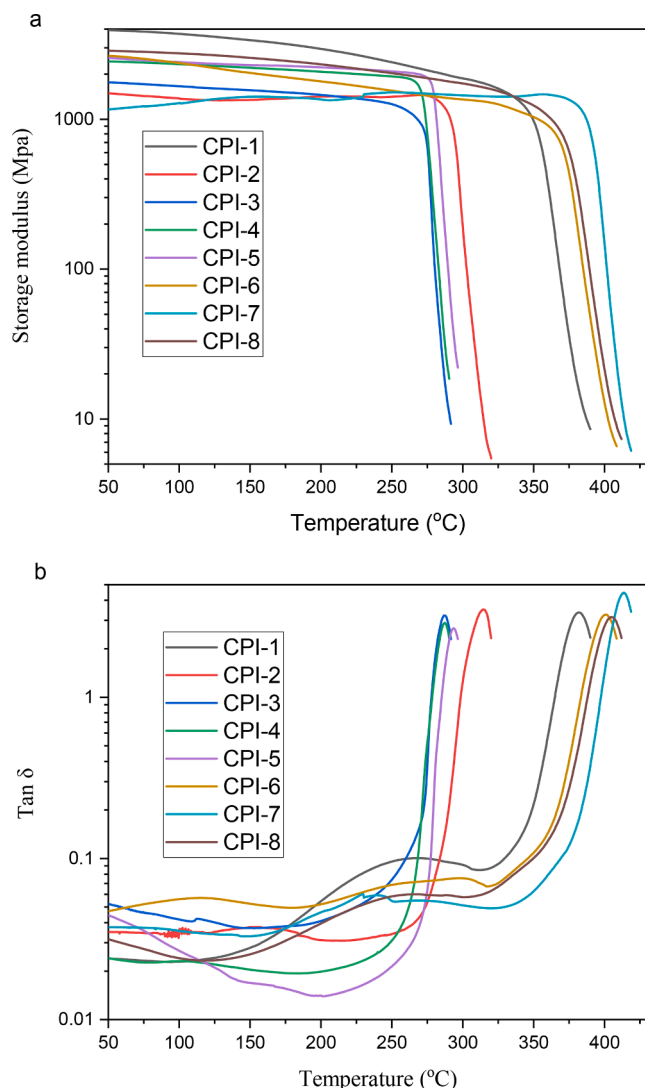


Fig. 4. DMA curves of 3,3'-BPDA-derived CPIs.

by TMA measurements. The in-plane CTE values of these CPIs were 61–72 ppm K⁻¹ (Table 2), which were comparable to those of 6FDA-derived ones. [3,39] The inferior dimensional stability of these CPIs can be attributed to their reduced linearity and suppressed CTC formations. CPI-4 (3,3'-BPDA/HFBAPP) and CPI-8 (3,3'-BPDA/TFMB/DABA) displayed the lowest CTE values because of their most compact chain packing or additional hydrogen bonding interactions, respectively.

3.5. Mechanical properties

3,3'-BPDA-derived CPIs exhibited tensile strengths of 63–93 MPa, modulus of 1.8–2.4 GPa, and elongation-at-break of 3.0–7.2% (Table 2 and Figure S2). These values were comparable or slightly inferior to those of 6FDA-derived CPIs except for apparently lower elongation-at-break [3,39–40]. The compromised mechanical properties of these CPIs could also be attributed to interrupted conjugation and loosened chain packing caused by the twisted 3,3'-BPDA residues and fluorinated substituents. The CPIs derived from flexible diamines showed higher tensile strengths and elongation-at-breaks despite their lower moduli. By comparison, CPIs from rigid diamines showed higher moduli but lower tensile strengths and elongation-at-breaks. However, the differences were marginal since their mechanical properties were governed by 3,3'-BPDA residues.

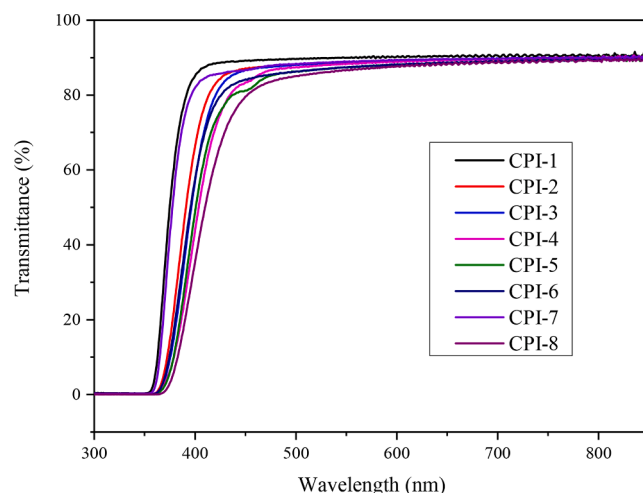


Fig. 5. UV-Vis spectra of 3,3'-BPDA-derived CPIs.

3.6. Optical properties

The CTC formation in the 3,3'-BPDA-derived CPIs was prohibited due to two facts. The first was the reduced inter- and intramolecular interactions caused by 3,3'-BPDA residues and fluorinated substituents. The second dealt with the weakened electron-donating capability of fluorinated diamine residues and reduced electron-withdrawing ability of the 3,3'-BPDA residues. As a result, these CPIs exhibited excellent optical transparency and light color (Figs. 5 and 6). According to the UV-vis spectra (Fig. 5), the cut-off wavelength and transmittance at 450 nm were 355–370 nm and 79.6–89.2%, respectively. Furthermore, these CPIs were colorless or pale yellow (Fig. 6), with *b** and yellow index values of 0.73–8.30 and 1.4–13.7, respectively (Table 3). A general correlation was observed between fluorine contents and optical properties. CPI-1 (3,3'-BPDA/TFMB) showed the best optical properties because of its highest fluorine content and largest interchain distance. CPI-7 (3,3'-BPDA/TFMB/FFDA) also displayed high optical transparency and low yellow index due to the unique cardo structure of fluorene. By comparison, 3,3'-BPDA/TFMB/DABA possessed the worst optical properties due to its lower fluorine content and possible discoloration of DABA during polymerization. For certain diamines, 3,3'-BPDA-derived CPIs displayed comparable or slightly inferior optical transparency than the 6FDA-derived ones owing to their lower fluorine contents. [3,39]

4. Conclusions

High-molecular-weight CPIs were successfully prepared from 3,3'-BPDA and fluorinated diamines via a one-step method. The combined effects of rigid and twisted 3,3'-BPDA residues, bulky CF₃ substituents, reduced electron-withdrawing ability of 3,3'-BPDA residues, and weakened electron-donating capability of fluorinated diamine residues endowed the CPIs with excellent optical transparency, outstanding thermal stability, high *T_g*, and good solubility. In particular, these CPIs showed *T₄₅₀* values of > 79%, *b* values of < 8.3 and *λ₀* of < 370 nm. Furthermore, the *T_g* and *T_{d5}* values of these polyimides were 287–414 °C and 516–579 °C, respectively. A strong correlation was observed between the chain rigidity and *T_g*, e.g. the CPIs with more flexible ether linkages exhibited lower *T_g* values. Meanwhile, the CPIs with higher fluorine contents exhibited better optical properties. 3,3'-BPDA-derived CPIs showed great potential in optical applications because of their excellent overall properties and possibly low cost. This work provides new insights on the development of CPIs using aromatic dianhydrides other than 6FDA.



Fig. 6. Images of 3,3'-BPDA-derived CPIs.

Table 3

Optical properties of 3,3'-BPDA-derived CPIs ^a.

CPI	Thickness (μm)	<i>L</i> [*]	<i>a</i> [*]	<i>b</i> [*]	YI ^b	Haze (%)	<i>T</i> ₄₅₀ (%) ^c	<i>λ</i> ₀ (nm)
CPI-1	27	95.8	−0.06	0.73	1.4	0.54	89.2	355
CPI-2	38	95.7	−0.39	1.67	2.9	0.62	87.1	363
CPI-3	35	95.4	−0.68	2.61	4.4	0.70	86.7	364
CPI-4	31	95.2	−1.57	4.90	8.0	0.55	83.4	364
CPI-5	33	94.7	−1.32	4.95	8.3	1.32	81.2	366
CPI-6	35	95.0	−1.74	5.01	8.1	0.65	81.9	368
CPI-7	38	95.2	−0.19	1.50	2.7	0.55	86.7	358
CPI-8	30	94.0	−2.31	8.30	13.7	0.64	79.6	370
6FDA-TFMB [39]	16						89.4	322
6FDA-DMBz [39]	15						86.2	342
6FDA-HFBAPP [3]	25					0.6	88	328

^a *L*^{*} refers to lightness. Positive *a*^{*} reflects red color, while negative *a*^{*} represents green color. Positive *b*^{*} reflects yellow color, while negative *b*^{*} represents blue color.

^b Yellowness index.

^c Transmittance at 450 nm.

CRedit authorship contribution statement

Yuanzhen Xu: Conceptualization, Investigation, Formal analysis, Writing – original draft. **Mengru Zhang:** Formal analysis, Writing – original draft, Writing – review & editing. **Yuanyuan Pang:** Formal analysis. **Tianyue Zheng:** Investigation, Writing – review & editing. **Li Zhang:** Investigation, Writing – review & editing. **Zhen Wang:** Investigation, Writing – review & editing. **Jingling Yan:** Conceptualization, Writing – original draft, Writing – review & editing, Supervision.

Declaration of Competing Interest

The authors declare that they have no known competing financial interests or personal relationships that could have appeared to influence the work reported in this paper.

Data availability

Data will be made available on request.

Acknowledgments

The authors are thankful to the Key Research & Development Program of Zhejiang Province (Nos. 2021C01186 and 2021C01126) and Joint Program of Jilin Province and Chinese Academy of Science (No. 2020SYHZ0001) for the financial support.

Appendix A. Supplementary data

Supplementary data to this article can be found online at <https://doi.org/10.1016/j.eurpolymj.2022.111528>.

References

- [1] I. Gouzman, E. Grossman, R. Verker, N. Atar, A. Bolker, N. Eliaz, Advances in Polyimide-Based Materials for Space Applications, *Adv. Mater.* 31 (2019) 1807738, <https://doi.org/10.1002/adma.201807738>.
- [2] J. Chen, C.T. Liu, Technology Advances in Flexible Displays and Substrates, *IEEE Access* 1 (2013) 150–158, <https://doi.org/10.1109/access.2013.2260792>.
- [3] H.-J. Ni, J.-G. Liu, Z.-H. Wang, S.-Y. Yang, A review on colorless and optically transparent polyimide films: Chemistry, process and engineering applications, *J. Ind. Eng. Chem.* 28 (2015) 16–27, <https://doi.org/10.1016/j.jiec.2015.03.013>.
- [4] C. Yi, W. Li, S. Shi, K. He, P. Ma, M. Chen, C. Yang, High-temperature-resistant and colorless polyimide: Preparations, properties, and applications, *Sol. Energy* 195 (2020) 340–354, <https://doi.org/10.1016/j.solener.2019.11.048>.
- [5] J.A. Kreuz, J.R. Edman, Polyimide Films, *Adv. Mater.* 10 (1998) 1229–1232, [https://doi.org/10.1002/\(sici\)1521-4095\(199810\)10:15<1229::aid-adma1229>3.0.co;2-b](https://doi.org/10.1002/(sici)1521-4095(199810)10:15<1229::aid-adma1229>3.0.co;2-b).
- [6] P.K. Tapaswi, C.-S. Ha, Recent Trends on Transparent Colorless Polyimides with Balanced Thermal and Optical Properties: Design and Synthesis, *Macromol. Chem. Phys.* 220 (2019) 1800313, <https://doi.org/10.1002/macp.201800313>.
- [7] M.-C. Choi, Y. Kim, C.-S. Ha, Polymers for flexible displays: From material selection to device applications, *Prog. Polym. Sci.* 33 (2008) 581–630, <https://doi.org/10.1016/j.progpolymsci.2007.11.004>.
- [8] Y. Zhuang, J.G. Seong, Y. Lee, M.: Polyimides containing aliphatic/alicyclic segments in the main chains, *Prog. Polym. Sci.* 92 (2019) 35–88, <https://doi.org/10.1016/j.progpolymsci.2019.01.004>.
- [9] S. Ando, T. Matsuura, S. Sasaki, Coloration of Aromatic Polyimides and Electronic Properties of Their Source Materials, *Polym. J.* 29 (1997) 69–76, <https://doi.org/10.1295/polymj.29.69>.
- [10] M. Hasegawa, K. Horie, Photophysics, photochemistry, and optical properties of polyimides, *Prog. Polym. Sci.* 26 (2001) 259–335, [https://doi.org/10.1016/s0079-6700\(00\)00042-3](https://doi.org/10.1016/s0079-6700(00)00042-3).
- [11] X. Hu, J. Yan, Y. Wang, H. Mu, Z. Wang, H. Cheng, F. Zhao, Z. Wang, Colorless polyimides derived from 2R,5R,7S,10S-naphthantetracarboxylic dianhydride, *Polym. Chem.* 8 (2017) 6165–6172, <https://doi.org/10.1039/c7py01048f>.
- [12] J. Miao, X. Hu, X. Wang, X. Meng, Z. Wang, J. Yan, Colorless polyimides derived from adamantane-containing diamines, *Polym. Chem.* 11 (2020) 6009–6016, <https://doi.org/10.1039/d0py01016b>.
- [13] M. Hasegawa, M. Fujii, J. Ishii, S. Yamaguchi, E. Takezawa, T. Kagayama, A. Ishikawa, Colorless polyimides derived from 1S,2S,4R,5R-cyclohexanetetracarboxylic dianhydride, self-orientation behavior during solution casting, and their optoelectronic applications, *Polymer* 55 (2014) 4693–4708, <https://doi.org/10.1016/j.polymer.2014.07.032>.
- [14] M. Hasegawa, T. Ishigami, J. Ishii, K. Sugiura, M. Fujii, Solution-processable transparent polyimides with low coefficients of thermal expansion and self-orientation behavior induced by solution casting, *Eur. Polym. J.* 49 (2013) 3657–3672, <https://doi.org/10.1016/j.eurpolymj.2013.08.002>.
- [15] H.T. Zuo, G.T. Qian, H.B. Li, F. Gan, Y.T. Fang, X.T. Li, J. Dong, X. Zhao, Q. H. Zhang, Reduced coefficient of linear thermal expansion for colorless and transparent polyimide by introducing rigid-rod amide units: synthesis and properties, *Polym. Chem.* 13 (2022) 2999–3008, <https://doi.org/10.1039/d2py00062h>.
- [16] M.-C. Choi, J. Wakita, C.-S. Ha, S. Ando, Highly Transparent and Refractive Polyimides with Controlled Molecular Structure by Chlorine Side Groups, *Macromolecules* 42 (2009) 5112–5120, <https://doi.org/10.1021/ma900104z>.
- [17] C.-P. Yang, Y.-Y. Su, Y.-C. Chen, Colorless poly(ether-imide)s deriving from 2,2-bis[4-(3,4-dicarboxyphenoxy)phenyl]propane dianhydride (BPADA) and aromatic bis

- (ether amine)s bearing pendent trifluoromethyl groups, *Eur. Polym. J.* 42 (2006) 721–732, <https://doi.org/10.1016/j.eurpolymj.2005.10.001>.
- [18] R. Lian, X. Lei, Y. Xiao, S. Xue, G. Xiong, Z. Zhang, D. Yan, Q. Zhang, Synthesis and properties of colorless copolyimides derived from 4,4'-diaminodiphenyl ether-based diamines with different substituents, *Polym. Chem.* 12 (2021) 4803–4811, <https://doi.org/10.1039/d1py00633a>.
- [19] S.-H. Hsiao, H.-M. Wang, W.-J. Chen, T.-M. Lee, C.-M. Leu, Synthesis and properties of novel triptycene-based polyimides, *J. Polym. Sci., Part A: Polym. Chem.* 49 (2011) 3109–3120, <https://doi.org/10.1002/pola.24748>.
- [20] L. Yi, C. Li, W. Huang, D. Yan, Soluble and transparent polyimides with high T_g from a new diamine containing tert-butyl and fluorene units, *J. Polym. Sci., Part A: Polym. Chem.* 54 (2016) 976–984, <https://doi.org/10.1002/pola.27933>.
- [21] H. Ozawa, E. Ishiguro, Y. Kyoya, Y. Kikuchi, T. Matsumoto, Colorless Polyimides Derived from an Alicyclic Tetracarboxylic Dianhydride, CpODA, *Polymers (Basel)* 13 (2021) 2824, <https://doi.org/10.3390/polym13162824>.
- [22] Z. Yang, H. Guo, C. Kang, L. Gao, Synthesis and characterization of amide-bridged colorless polyimide films with low CTE and high optical performance for flexible OLED displays, *Polym. Chem.* 12 (2021) 5364–5376, <https://doi.org/10.1039/d1py00762a>.
- [23] R.E. Southward, D.S. Thompson, T.A. Thornton, D.W. Thompson, A.K. St. Clair, Enhancement of Dimensional Stability in Soluble Fluorinated Polyimides via the in Situ Formation of Lanthanum(III)–Oxo–Polyimide Nanocomposites, *Chem. Mater.* 10 (1998) 486–494, <https://doi.org/10.1021/cm970386l>.
- [24] H. Lao, N. Mushtaq, G. Chen, B. Wang, Y. Ba, X. Fang, Synthesis and properties of transparent random and multi-block polyamide-imide films with high modulus and low CTE, *Eur. Polym. J.* 153 (2021), 110512, <https://doi.org/10.1016/j.eurpolymj.2021.110512>.
- [25] P.K. Tapaswi, M.-C. Choi, S. Nagappan, C.-S. Ha, Synthesis and characterization of highly transparent and hydrophobic fluorinated polyimides derived from perfluorodecylthio substituted diamine monomers, *J. Polym. Sci., Part A: Polym. Chem.* 53 (2015) 479–488, <https://doi.org/10.1002/pola.27461>.
- [26] X.-H. Yu, J.-N. Liu, D.-Y. Wu, Colorless PI structure design and evaluation for achieving low CTE target, *Mater. Today Commun.* 21 (2019), 100562, <https://doi.org/10.1016/j.mtcomm.2019.100562>.
- [27] G. Song, C. Chen, Colorless, heat resistant polyimide films derived from 2,3,3',4'-biphenyltetracarboxylic dianhydride, *IOP Conf. Ser.: Mater. Sci. Eng.* 733 (1) (2020) 012035, <https://doi.org/10.1088/1757-899x/733/1/012035>.
- [28] Brian C. Auman D. P. H., Kirby V. Scherer Jr, Elizabeth F. McCord and William H. Shaw Jr Synthesis of a new fluoroalkylated diamine, 5-[1 H,1 H-2-bis (trifluoromethyl)-heptafluoropentyl]-1,3-phenylenediamine, and polyimides prepared therefrom *Polymer*, 36 (1995) 651–656. [https://doi.org/10.1016/0021-8995\(95\)00111-1](https://doi.org/10.1016/0021-8995(95)00111-1).
- [29] F. Li, J. Liu, X. Liu, Y. Wang, X. Gao, X. Meng, G. Tu, High Performance Soluble Polyimides from Ladder-Type Fluorinated Dianhydride with Polymorphism, *Polymers (Basel)* 10 (2018) 546, <https://doi.org/10.3390/polym10050546>.
- [30] S. Ando, M. Ueda, M. Kagimoto, M. Kochi, T. Takeichi, M. Hasegawa, *The latest polyimides: fundamentals and applications*, second ed., NYS, Tokyo, 2010, pp. 102–128.
- [31] Y.J. Tong, W.X. Huang, J. Luo, M.X. Ding, Synthesis and properties of aromatic polyimides derived from 2,2',3,3'-biphenyltetracarboxylic dianhydride, *J. Polym. Sci., Part A: Polym. Chem.* 37 (1999) 1425–1433, [https://doi.org/10.1002/\(SICI\)1099-0518\(19990515\)37:10<1425::AID-POLA4>3.0.CO;2-G](https://doi.org/10.1002/(SICI)1099-0518(19990515)37:10<1425::AID-POLA4>3.0.CO;2-G).
- [32] I. Rozhanskii, K.O.K. Goto, Synthesis and properties of polyimides derived from isomeric biphenyltetracarboxylic dianhydrides, *Polymer* 41 (2000) 7057–7065, [https://doi.org/10.1016/S0032-3861\(00\)00068-9](https://doi.org/10.1016/S0032-3861(00)00068-9).
- [33] H. Zhou, C. Chen, R. Kanbara, T. Sasaki, R. Yokota, Synthesis and Properties of Copolyimides Derived from Isometric Biphenyltetracarboxylic Dianhydrides (a-BPDA and i-BPDA) and Oxydiphthalic Dianhydride (ODPA) with 4,4'-Oxydianiline (4,4'-ODA), *High Perform. Polym.* 17 (2016) 213–224, <https://doi.org/10.1177/0954008305044856>.
- [34] H. Zhou, C. Chen, R. Kanbara, T. Sasaki, R. Yokota, Isomeric Dianhydrides Based Modified Phenylethynyl-terminated Addition-type Imide Oligomers, *High Perform. Polym.* 17 (2016) 193–212, <https://doi.org/10.1177/0954008305044855>.
- [35] M. Kochi, C. Chen, R. Yokota, M. Hasegawa, P. Hergenrother, Isomeric Biphenyl Polyimides. (II) Glass Transitions and Secondary Relaxation Processes, *High Perform. Polym.* 17 (2016) 335–347, <https://doi.org/10.1177/0954008305055557>.
- [36] J. Yan, Z. Wang, L. Gao, M. Ding, X.: Polyimides Derived from 3,3'-Bis(N-aminophthalimide), *Macromolecules* 39 (22) (2006) 7555–7560.
- [37] X. Meng, G. Lu, X. Liu, Q. Meng, J. Shi, H. Yuan, H. Ke, X. Wang, W. Fan, J. Liu, J. Yan, Z. Wang, Highly Soluble Phenylethynyl-terminated Imide Oligomers and Thermosetting Polyimides Based on 2,2',3,3'-Biphenyltetracarboxylic Dianhydride, *Chem. Res. Chin. Univ.* 35 (2019) 530–536, <https://doi.org/10.1007/s40242-019-8334-z>.
- [38] L. Zhai, S. Yang, L. Fan, Preparation and characterization of highly transparent and colorless semi-aromatic polyimide films derived from alicyclic dianhydride and aromatic diamines, *Polymer* 53 (2012) 3529–3539, <https://doi.org/10.1016/j.polymer.2012.05.047>.
- [39] W.F. Peng, H.Y. Lei, X.X. Zhang, L.H. Qiu, M.J. Huang, Fluorine substitution effect on the material properties in transparent aromatic polyimides, *Chinese J. Polym. Sci.* 40 (2022) 781–788, <https://doi.org/10.1007/s10118-022-2702-8>.
- [40] P.M. Hergenrother, K.A. Watson, J.G. Smith, J.W. Connell, R. Yokota, Polyimides from 2,3,3',4'-biphenyltetracarboxylic dianhydride and aromatic diamines, *Polymer* 43 (19) (2002) 5077–5093.